# The influenza A virus host shutoff factor PA-X is rapidly turned over in a strain-specific manner

Rachel Emily Levene[a,b], Shailab D. Shrestha[a,b], Marta Maria Gaglia[a,b #]

[a]Graduate Program in Molecular Microbiology, Tufts University Graduate School of Biomedical Sciences, Boston, MA, USA

[b]Department of Molecular Biology and Microbiology, Tufts University School of Medicine, Boston, MA, USA

[#]Send correspondence to:

Marta Maria Gaglia (marta.gaglia@tufts.edu)

**Key Words:** influenza A virus, PA-X, host shutoff, protein turnover

**Running Title:** The influenza A virus RNase PA-X is unstable

**Abstract Word Count: 202**

**Main Text Word Count: 6261**

**ABSTRACT:**

The influenza A endoribonuclease PA-X regulates virulence and transmission of the virus by reducing host gene expression and thus regulating immune responses to influenza A virus. Despite this key function in viral biology, the levels of PA-X protein remain markedly low during infection, and previous results suggest that these low levels are not solely the result of regulation of the level of translation and RNA stability. How PA-X is regulated post-translationally remains unknown. We now report that the PA-X protein is rapidly turned over. PA-X from multiple viral strains are short-lived, although the half-life of PA-X ranges from ~30 minutes to ~3.5 hours depending on the strain. Moreover, sequences in the variable PA-X C-terminal domain are primarily responsible for regulating PA-X half-life, although the N-terminal domain also accounts for some differences among strains. Interestingly, we find that the PA-X from the 2009 pandemic H1N1 strain has a longer half-life compared to the other variants we tested. This PA-X isoform has been reported to have a higher host shutoff activity, suggesting a role for protein turnover in regulating PA-X activity. Collectively, this study reveals a novel regulatory mechanism of PA-X protein levels that may impact host shutoff activity during influenza A virus infection.

34 **IMPORTANCE**

35 The PA-X protein from influenza A virus reduces host immune responses to infection through
36 suppressing host gene expression, including genes encoding the antiviral response. Thus, it plays
37 a central role in influenza A virus biology. Despite its key function, PA-X was only discovered
38 in 2012 and much remains to be learned including how PA-X activity is regulated to promote
39 optimal levels of viral infection. In this study, we reveal that PA-X protein levels are very low
40 likely because of rapid turnover. We show that instability is a conserved property among PA-X
41 variants from different strains of influenza A virus, but that the half-lives of PA-X variants
42 differ. Moreover, the longer half-life of PA-X from the 2009 pandemic H1N1 strain correlates
43 with its reported higher activity. Therefore, PA-X stability may be a way to regulate its activity
44 and may contribute to the differential virulence of influenza A virus strains.

45 **INTRODUCTION:**

46 Viruses employ multiple strategies to block host antiviral defenses. In many viruses, this
47 inhibition is partly achieved through a blockade of host gene expression, a process termed "host
48 shutoff". One of the ways influenza A virus induces host shutoff is through the activity of a viral
49 endoribonuclease (RNase), PA-X (1–3). The RNase activity of PA-X results in global changes in
50 the cellular transcriptome (3, 4), while viral mRNAs and genomic RNAs escape PA-X
51 degradation (5). Influenza A viruses engineered to lack PA-X trigger a more potent innate
52 immune and inflammatory response in mice, chickens, and pigs, presumably because of
53 decreased host shutoff (1, 6–10). These results indicate that PA-X controls immune responses *in*
54 *vivo.* More recently, a role for PA-X in transmission has also been established (11, 12). Despite
55 its clear *in vivo* role, much remains to be determined about PA-X biology during infection. PA-X
56 was discovered in 2012 and studies to date have primarily focused on dissecting its mechanism
57 of action, including how subsets of RNAs, including viral RNAs, escape PA-X degradation.
58 Whether and how PA-X activity itself is regulated has not been explored in detail. One study
59 found that co-translational N-terminal acetylation is required for PA-X host shutoff activity (13),
60 but whether there are other co- and post-translational regulatory mechanisms remains unknown.
61 Interestingly, prolonged PA-X expression may be cytotoxic, as shown in yeast (13, 14). While
62 this is not surprising given its widespread downregulation of RNAs, this observation underscores
63 the idea that PA-X activity may need to be regulated during infection to prevent premature death
64 of the infected cells.

65

66 One way to regulate or limit PA-X activity could be to keep pools of active PA-X protein low in
67 the infected cell. Indeed, PA-X protein levels are remarkably low during infection. Metabolic

68 labeling of nascent proteins in influenza A virus infected cells showed that the levels of PA-X
69 are barely above the limit of detection and lower than other influenza proteins, including the
70 well-known host shutoff factor NS1 (1). These low levels are in part due to how PA-X is
71 produced. PA-X production requires a programmed +1 ribosomal frameshift during translation of
72 segment 3, which encodes the polymerase acidic (PA) subunit of the viral RNA dependent RNA
73 polymerase (RdRp) (1, 15). Only a small percentage of translational runs result in frameshifting
74 and produce PA-X, which has the same N-terminal RNase domain as PA (PA-X amino acids (aa)
75 1-191) and a unique C-terminal domain known as the "X-ORF" (PA-X aa 192-232 or 192-252
76 depending on the strain) (1, 16). Of note, despite this non-canonical production mechanism, PA-
77 X is present in all influenza A virus isolates (16), which underscores its importance in influenza
78 A virus biology. However, the mechanism of PA-X production does not entirely explain the low
79 levels of PA-X. Indeed, PA-X levels are also low or undetectable when PA-X is expressed
80 ectopically (17). In these experiments, a single nucleotide has been deleted in the expression
81 construct to mimic the frameshift and all translational runs produce PA-X (17). The low levels
82 are also not because PA-X degrades its own mRNA, as mutating the PA-X catalytic residues
83 D108 or K134 in this ectopic expression system does not increase PA-X levels dramatically (3,
84 17). This suggests that PA-X levels may be regulated at the level of protein stability.
85
86 Regulation of stability is a well-established post-translational mechanism of protein regulation.
87 For example, Kosik *et. al* showed that protein turnover regulates the immunomodulatory activity
88 of PB1-F2, another influenza A virus virulence factor (18). PB1-F2 inhibits induction of the
89 antiviral cytokine interferon beta (IFN-β) and increases the activity of the viral RdRp (19–21).
90 Mutating the residues required for PB1-F2 ubiquitination and rapid turnover increases PB1-F2

91 protein levels, which results in a stronger inhibition of IFN-β induction (18). Similarly,
92 regulation of PA-X at the level of protein stability could modulate the host shutoff activity of
93 influenza A virus.
94
95 Previous observations suggest that the X-ORF may regulate the levels of the PA-X protein, as
96 ectopic expression of the N-terminal domain of PA-X results in much higher protein levels than
97 ectopic expression of either wild type (wt) or catalytically inactive PA-X (17). This is not due to
98 changes in frameshifting, as this ectopic expression construct has a nucleotide deletion to mimic
99 the frameshift and only encodes PA-X. A role for the X-ORF in post-translational control of PA-
100 X levels and activity would explain why almost all influenza A strains encode a PA-X protein
101 that has a 61 or 41-aa X-ORF (16) even though only the first 15 aa of the X-ORF are required for
102 PA-X shutoff activity in cells (3, 17, 22). Moreover, most of the sequence variation among PA-X
103 from different strains occurs after the 15th amino acid of the X-ORF, and the strength of PA-X
104 activity has been reported to vary among strains (17, 23, 24).
105
106 Here we report the first investigation of post-translational regulation of PA-X protein levels. We
107 find that PA-X is markedly unstable and identify a region of the A/Puerto Rico/8/1934 H1N1
108 (PR8) X-ORF that regulates PA-X turnover. Additionally, we find that the half-life of PA-X
109 differs among strains, even though all the PA-X variants tested have generally short half-lives.
110 Interestingly, of the variants we tested, PA-X from the 2009 pandemic H1N1 strain had the
111 longest half-life, which may explain its reported higher host shutoff activity (17, 23, 24). Thus,
112 modulation of PA-X stability may be a mechanism used to regulate PA-X host shutoff activity in
113 different strains and may contribute to influenza A pathogenesis.

114

115 **RESULTS**

116 **PA-X is unstable**

117 Several observations suggested to us that PA-X may be unstable. PA-X is expressed at low levels
118 not only during infection (1), but also during ectopic overexpression from a high expression
119 CMV promoter [(17), our unpublished observations]. Furthermore, ectopic overexpression of the
120 N-terminal RNase domain from the same high expression CMV promoter results in much higher
121 protein levels (17). While the RNase domain in isolation is inactive in cells (3, 5, 17, 22), the
122 differences in protein levels are not due to the loss of activity, because expressing a catalytically
123 inactive version of PA-X still results in markedly low PA-X expression levels (3, 17). Thus, we
124 sought to directly test if PA-X is rapidly turned over. To determine the half-life of the PA-X
125 protein, we performed a cycloheximide chase in human embryonic kidney (HEK) 293T cells
126 transfected with a C-terminally myc tagged PA-X from the influenza A virus strain A/Puerto
127 Rico/8/1934 H1N1 (PR8) containing the D108A mutation in the RNase active site. This mutation
128 abolishes PA-X catalytic activity and host shutoff function (3, 5). We used catalytically inactive
129 PA-X for this experiment and throughout this study to eliminate any confound from changes in
130 host gene expression or PA-X mRNA levels as a result of PA-X activity. Additionally, to make
131 sure any differences in PA-X protein levels are due to changes in turnover and not frameshifting,
132 in this experiment and throughout this study we used PA-X expression constructs where all
133 translational runs produce PA-X, as a single nucleotide was deleted to mimic the frameshift.
134 After treating PA-X-expressing cells with cycloheximide to inhibit translation, we analyzed PA-
135 X protein levels at 0, 15, 30, 60, and 120 minutes after cycloheximide addition by western
136 blotting. Strikingly, PA-X protein levels decreased dramatically one hour after the addition of

137 cycloheximide (Fig 1A and 1B), suggesting that PA-X is markedly unstable. By contrast, levels
138 of PA-X mRNA did not decrease throughout the cycloheximide time course (Fig 1C),
139 confirming that the decrease in PA-X protein levels is not due to changes in transcript levels.
140 Based on regression analysis, we calculated a half-life of 86 minutes for PR8 PA-X (Fig 1B,
141 Table 1). This is short compared to the half-life of other influenza proteins. For example, the
142 immune evasion factor NS1 from PR8 has a half-life of over 24 hours (25) and PR8 PB1-F2 has
143 a half-life of 6.5 hours (26). In addition, human proteins have a median half-life of 8.7 hours
144 (27). Together, these data show that PA-X is rapidly turned over compared to other viral and host
145 proteins.
146
147 **PA-X host shutoff activity in infected cells is reduced upon translational inhibition**
148 To confirm that PA-X is unstable in the context of influenza A virus infection we first attempted
149 to measure its half-life in PR8-infected cells using an antibody against PR8 PA that has been
150 previously used to detect PR8 PA-X (28). However, like Rigby *et al.* (28), we observed multiple
151 bands in the section of the blot corresponding to the predicted molecular weight of PA-X, and
152 were unable to reliably and reproducibly identify the band corresponding to PA-X.
153 Unfortunately, we cannot tag PA-X in the context of the virus. The C-terminus cannot be tagged
154 because it overlaps with the coding sequence for the C-terminus of PA (1, 15). N-terminal tags
155 reduce PA activity and viral replication (29, 30), and are also expected to reduce the activity of
156 PA-X because of the importance of its N-terminal acetylation (13). Therefore, we sought another
157 way to look for evidence of PA-X instability during infection and used PA-X activity in the
158 presence of cycloheximide as a proxy for rapid changes in PA-X protein levels. We reasoned that
159 if levels of PA-X are quickly depleted after halting translation with cycloheximide, there will be

160 less PA-X host shutoff activity in cells. To confirm this, we first tested PA-X host shutoff
161 activity in the presence of cycloheximide in A549 cells that inducibly express either wt PR8 PA-
162 X or the catalytically inactive PR8 PA-X D108A mutant. These cells allow us to reliably
163 measure PA-X-dependent changes in the RNA levels of endogenous genes (3, 5). Following
164 overnight induction of PA-X expression and a subsequent 2-hour cycloheximide treatment, we
165 analyzed levels of G6PD and TAF7 mRNA, which are representative PA-X target and resistant
166 RNAs, respectively (3). Levels of G6PD significantly decreased upon PA-X expression in
167 vehicle-treated cells (Fig 2A). In contrast, there was no statistically significant decrease in G6PD
168 levels in PA-X-expressing cells treated with cycloheximide (Fig 2A). We note that there was
169 substantial experimental variability in cycloheximide-treated cells, perhaps due to different
170 levels of PA-X mRNA or of residual PA-X protein after treatment (Fig 2A). Nonetheless,
171 cycloheximide had no effect on the levels of G6PD in cells expressing catalytically inactive PA-
172 X or levels of the PA-X resistant RNA TAF7 (Fig 2A), confirming that the effect of
173 cycloheximide on RNA levels was at least partially linked to PA-X activity. Furthermore, PA-X
174 mRNA levels did not decrease with cycloheximide (Fig 2A), confirming that any decrease in
175 PA-X host shutoff activity is not the result of a decrease in PA-X transcript levels.
176
177 We then performed the same experiment in A549 cells infected with either wt PR8 or PA-X-
178 deficient PR8 virus (ΔX). PR8 ΔX carries mutations in the frameshifting site in segment 3 that
179 reduce PA-X production, as well as a nonsense mutation at PA-X aa 201, which abolishes
180 activity of any residual PA-X (3). At 24 hours post-infection, we analyzed levels of G6PD and
181 TAF7 mRNA after a 2-hour cycloheximide treatment. As expected, G6PD levels were
182 significantly lower in wt PR8-infected cells compared to PR8 ΔX-infected cells due to PA-X

183 mediated host shutoff, while the levels of the PA-X-resistant RNA TAF7 were similar (Fig 2B).
184 However, there was no significant difference in G6PD levels in wt PR8 *vs.* PR8 ΔX-infected
185 cells after treatment with cycloheximide (Fig 2B). This result suggests that cycloheximide
186 treatment prevents PA-X-mediated host shutoff, presumably due to a rapid decrease in PA-X
187 protein levels. As expected, PA-X had no effect on TAF7 levels (Fig 2B). There were no
188 significant changes in the RNA levels of the viral gene HA during cycloheximide treatment (Fig
189 2B), confirming that the decrease in PA-X activity is not the result of changes in viral
190 replication. Thus, while we cannot examine changes in PA-X protein levels in infected cells and
191 test its protein stability, we do observe markedly reduced PA-X activity after translation is
192 inhibited. Taken together with the short half-life of PR8 PA-X (Fig 1) and the decrease in its
193 activity after translational block during ectopic expression (Fig 2A), our results indicate that the
194 reduced PA-X activity after translational block during infection is likely the result of decreased
195 PA-X protein levels. Therefore, it is likely that PA-X is rapidly turned over during infection.
196

197 **PA-X-myc is unstable in influenza A virus-infected cells**

198 Because we were unable to reliably detect PA-X during infection and there was some variability
199 in measuring PA-X activity as a proxy for rapid changes in PA-X protein levels (Fig 2A), we
200 sought an additional way to look for evidence of PA-X instability during infection. Thus, we
201 measured the stability of ectopically expressed PA-X in mock or wt PR8-infected cells. For this
202 experiment, we used HEK 293T cells that inducibly express C-terminally myc tagged
203 catalytically inactive PR8 PA-X (HEK 293T-iPA-X_PR8_D108A), infected them for 18 hours
204 and then treated them with cycloheximide to inhibit translation. As expected based on our
205 previous results, PA-X-myc protein levels significantly decreased in both mock and wt PR8-

206 infected cells following a 2-hour cycloheximide treatment (Fig 2C and 2D). In contrast, there
207 were no significant changes in the levels of the virus-encoded M1 protein between vehicle- and
208 cycloheximide-treated wt PR8-infected cells (Fig 2C and 2E), indicating that changes in PA-X-
209 myc protein levels were not due to changes in viral replication. Thus, ectopically expressed PA-
210 X-myc is rapidly turned over in infected cells, which is consistent with the idea that virus-
211 encoded PA-X is also unstable under these conditions.
212
213 **The half-life of PA-X varies among influenza A virus strains**
214 Although all influenza A virus strains are predicted to encode PA-X, the sequence of PA-X
215 varies across strains (16). Thus, we sought to determine whether the instability we observed in
216 PR8 PA-X was conserved in PA-X from other strains of influenza A virus. We created
217 catalytically inactive D108A mutants of the PA-X from the 2009 pandemic H1N1 strain
218 A/California/7/2009pdm (pH1N1), the lab-adapted H3N2 strain A/Udorn/307/1972 (Udorn), the
219 seasonal H3N2 strain A/Perth/16/2009 (Perth), and the pre-pandemic seasonal H1N1 strain
220 A/Hong Kong/218847/2006 (HK06), all with a C-terminal myc tag. Fusing all variants to the
221 same tag allows us to better compare protein levels among strains, since many antibodies against
222 influenza proteins only recognize a particular strain or serotype. Udorn and HK06 PA-X were as
223 or more unstable than PR8 PA-X, with half-lives of 34 and 83 minutes, respectively (Fig 3A, 3B,
224 3D, 3E, Table 1). In contrast, Perth PA-X was more stable than PR8 PA-X, with a half-life of
225 156 minutes (Fig 3G, 3H, Table 1). pH1N1 PA-X was also significantly more stable than its PR8
226 counterpart, with a half-life of 207 minutes (Fig 3J, 3K, Table 1). Importantly, the longer lived
227 PA-X variants (Perth and pH1N1 PA-X) still have a shorter half-life than the average human
228 protein (~9 hrs) (27), suggesting they are still relatively unstable. Also, there were no significant

229 decreases in mRNA levels of PA-X from any of the strains during the cycloheximide time
230 courses (Fig 3C, 3F, 3I, 3L), confirming that the decrease in PA-X protein levels is not due to
231 changes in transcript levels. Together, these data show that instability is a conserved property
232 among PA-X variants, but that there are differences in PA-X half-life among strains. Moreover,
233 the pH1N1 PA-X is substantially longer lived than other variants.
234
235 **Amino acids 17-41 of the X-ORF contribute to regulation of PA-X instability**
236 Because ectopic overexpression of the N-terminal domain of PA-X results in higher protein
237 levels than overexpression of full length PA-X (17), we tested whether the X-ORF regulates PA-
238 X stability. We took two complementary approaches: we fused the PR8 X-ORF to the stable
239 reporter protein dsRed ("dsRed-XORF") to test whether the X-ORF reduces DsRed stability and
240 we truncated the X-ORF in PR8 PA-X to test whether this increases PA-X stability. We observed
241 that levels of dsRed-XORF significantly decreased after six hours of cycloheximide treatment,
242 whereas levels of dsRed remained constant (Fig 4A-B). There was no decrease in mRNA levels
243 of dsRed or dsRed-XORF upon cycloheximide treatment (Fig 4C), confirming that decreases in
244 dsRed protein levels are not due to changes in transcript levels. This indicates that addition of the
245 X-ORF can reduce stability of an unrelated protein. To test the effect of X-ORF truncations, we
246 chose to test a truncated version that ended after aa 16 of the X-ORF in PR8 PA-X ("PA-X16",
247 Fig 4D), because truncation of the entire X-ORF results in loss of nuclear localization of PA-X
248 and host shutoff activity in cells (5, 17). In contrast, PA-X mutants retaining at least 15 aa of the
249 X-ORF are primarily localized to the nucleus, like full-length PA-X (17) and have wild-type host
250 shutoff activity (3, 17, 22). Thus, using the PA-X16 truncation should exclude potential
251 confounding factors, such as changes in subcellular localization or in protein-protein interactions

252 needed for activity. In contrast to the rapid decrease in the levels of full-length PA-X (PA-X61)
253 after cycloheximide addition, the protein levels of PA-X16 remained constant throughout the
254 two-hour time course (Fig 4E and 4F). There were also no significant changes in the mRNA
255 levels of PA-X16 throughout the time course (Fig 4G). Thus, the truncated PA-X16 is more
256 stable than the full-length protein. Together, these data show that the X-ORF, in particular
257 sequences in the X-ORF after the 16$^{th}$ residue, contains sequences that reduce protein stability
258 and contribute to the instability of PA-X. Since the first 15 amino acids of the X-ORF are
259 necessary and sufficient for host shutoff activity (3, 17, 22), these data also suggest that the
260 portions of the X-ORF involved in mediating host shutoff activity and stability are different.
261
262 While the first 15 aa of the X-ORF are generally conserved among strains, the sequences after
263 the 16th aa vary. In particular, there are two main variants of PA-X in influenza A strains, which
264 are distinguishable by their protein lengths: one is 252-aa long, with an X-ORF of 61 aa, and the
265 other is 232-aa long, with an X-ORF of 41 aa (16). The PA-X variants in PR8, Perth, Udorn and
266 HK06 all have a 61-aa X-ORF, like most human strains, while the pH1N1 PA-X has a 41-aa X-
267 ORF, which is otherwise found in a subset of swine and canine strains (16). Although some
268 studies have suggested that the length of the X-ORF may regulate activity (12, 31–33), it is still
269 unclear exactly what the function of the additional 20 aa is. Since pH1N1 PA-X has a much
270 longer half-life than most of the other PA-X isoforms we tested (Fig 3K, Table 1), we wondered
271 if the shorter X-ORF accounted for the difference in stability. We thus measured the half-life of a
272 truncated version of catalytically inactive PR8 PA-X that ended after the 41st amino acid with a
273 C-terminal myc tag, which we termed "PA-X41" (Fig 4H). Despite the truncation, PR8 PA-X41
274 protein levels rapidly decreased after translation inhibition (Fig 4I and 4J), with a half-life of 99

275 minutes. This is not significantly different from that of full length PR8 PA-X (PA-X61) ($p$ =
276 0.8118) (Fig 4J). We note that we consistently detected a double band in cells expressing PR8
277 PA-X41. While the reason for this doublet is currently unknown, a similar doublet was also
278 apparent in the staining for pH1N1 PA-X in Hayashi *et al.* (17). There were no significant
279 decreases in the mRNA levels of PR8 PA-X41 (Fig 4K), confirming that the decrease in PR8
280 PA-X41 protein levels is not due to changes in transcript levels. Thus, the distal 20 residues of
281 PR8 PA-X likely do not play a role in PR8 PA-X's rapid turnover and other sequence differences
282 between PR8 and pH1N1 PA-X are responsible for their different turnover rates. Together, these
283 data show that the region contributing PA-X instability is located between the 17$^{th}$ and 41$^{st}$ aa.
284
285 **PA-X amino acid 220 plays a role in protein turnover**
286 Since sequences between PA-X aa 208 and aa 232 (X-ORF aa 17-41) appeared to control PA-X
287 stability, we performed an alignment of the X-ORF of PA-X from the strains we tested.
288 Although there were several amino acids that varied between the sequences, only one amino acid
289 changed in a way that was consistent with the protein half-life, aa 220. In the longer-lived PA-X
290 variants (Perth and pH1N1) this residue is a histidine, whereas in the shorter-lived PA-X variants
291 (PR8, Udorn, HK06), this residue is an arginine (Fig 5A). Interestingly, this is one of only eight
292 amino acid differences between the Udorn and Perth PA-X, which come from H3N2 strains
293 collected almost 40 years apart and have very different half-lives in our assays (Fig 3). To
294 determine if aa 220 plays a role in PA-X turnover, we introduced an R220H mutation in PR8
295 PA-X and a H220R mutation in pH1N1 PA-X. Upon a 2-hour treatment with cycloheximide, the
296 protein levels of wt PR8 PA-X significantly decreased, but levels of PR8 PA-X R220H remained
297 stable (Fig 5B and 5C). Conversely, levels of wt pH1N1 PA-X remained stable, but the levels of

298 pH1N1 PA-X H220R decreased, although the change did not reach statistical significance (Fig
299 5E and 5F). As expected, there was no significant decrease in the mRNA levels of any of the PA-
300 X variants in cells treated with cycloheximide (Fig 5D and 5G). Together these data point to a
301 role for aa 220 in controlling PA-X turnover.
302
303 **The N-terminal domain of PA-X also has a role in PA-X stability**
304 To further examine how the different X-ORF variants of PR8 and pH1N1 affect PA-X stability,
305 we created three different PR8 PA-X/pH1N1 PA-X chimeras and tested their stabilities. We
306 extended the X-ORF of pH1N1 PA-X to 61 aa with the 20 distal residues of the PR8 X-ORF
307 (pH1N1-X61), and we also swapped the X-ORFs of PR8 PA-X and pH1N1 PA-X (Fig 6A).
308 Addition of the 20 distal residues of PR8 did not reduce pH1N1 stability, as pH1N1-X61 protein
309 levels remained stable after 2 hours of cycloheximide treatment (Fig 6B and 6C), confirming that
310 the 20 distal residues do not drive rapid turnover of PR8 PA-X. However, addition of the entire
311 PR8 X-ORF to the pH1N1 RNase domain (pH1N1-PR8) also did not reduce the stability of the
312 protein to the levels of PR8 PA-X after 2 hours of cycloheximide treatment (Fig 6E and 6F). In
313 both cases, we saw a similar pattern of stability using a 4-hour cycloheximide treatment (data not
314 shown). Furthermore, addition of the pH1N1 X-ORF to the PR8 RNase domain (PR8-pH1N1)
315 did not increase its stability, as its protein levels still significantly decreased after 2 hours of
316 cycloheximide (Fig 6E and 6F). In all cases there were no significant decreases in PA-X mRNA
317 between vehicle- and cycloheximide-treated cells, confirming that any decrease in protein levels
318 is not due to changes at the transcript level (Fig 6D and 6G). While these data are consistent with
319 the idea that the 20-aa truncation is not responsible for the higher stability of pH1N1 PA-X, they
320 also suggest that X-ORF sequences alone do not explain all the differences in turnover between

321 PR8 and pH1N1 PA-X. We conclude that both the X-ORF and the N-terminal RNase domain
322 have a role in controlling PA-X turnover rates.
323
324 **DISCUSSION**
325 The PA-X protein is present at low levels in influenza A virus-infected cells, which has been
326 generally assumed to be due to its production mechanism based on ribosomal frameshifting.
327 However, here we report that PA-X protein levels are also regulated at the post-translational
328 level, and that PA-X is rapidly turned over (Fig 1-3). Results for host shutoff activity in PR8-
329 infected cells suggest that PR8 PA-X is also unstable during infection and that the short half-life
330 is not an artifact of ectopic expression (Fig 2). Moreover, protein instability is a conserved
331 property of PA-X, because all of the PA-X variants we tested from different influenza A viruses
332 have short half-lives, ranging from ~30 minutes (Udorn PA-X) to ~3.5 hours (pH1N1 PA-X)
333 (Fig 3). At least some of the determinants of protein stability are located in the X-ORF of the
334 protein, because truncation of the X-ORF to 16 aa significantly increases stability and fusion to
335 the X-ORF is sufficient to induce turnover of an unrelated protein (Fig 4). Moreover, sequences
336 between PA-X aa 208-232 (aa 17-41 of the X-ORF) and aa 220 (aa 29 of the X-ORF) in
337 particular appear to be crucial for PA-X turnover. Truncating PA-X at aa 232 does not change its
338 half-life (Fig 4J), while truncating it at aa 207 significantly increases it (Fig 4F), and switching
339 aa 220 between a histidine and an arginine changes PA-X stability (Fig 5). However, the N-
340 terminal RNase domain also has a role in PA-X turnover, as swapping the X-ORFs of
341 PR8/pH1N1 is not sufficient to alter their stability (Fig 6). We propose that the purpose of this
342 post-translational regulation of PA-X is to maintain low steady-state levels of the protein in
343 infected cells, which in turn may limit the active pool of PA-X. Given that PA-X is already made

344 at low levels during infection, the instability of this protein suggests that limiting PA-X activity
345 is of paramount importance for viral replication.
346
347 It is attractive to think that the rapid turnover of active PA-X in the cell could serve as a
348 mechanism to control PA-X host shutoff activity. Prolonged PA-X activity could in theory have
349 catastrophic consequences not only for the cell but also for successful viral infection. We have
350 observed that prolonged PA-X expression kills human cells (data not shown), as reported in
351 yeast (13, 14). This cytopathic effect could be due to the activation of cellular stress response
352 pathways as a response to prolonged widespread RNA degradation, or to a direct effect of the
353 RNA degradation on the levels of unstable proteins that keep the cell alive, like the Bcl-2 family
354 member MCL-1 (34). During infection, this toxicity could prematurely kill the infected cell
355 before progeny virions are made, which would curtail viral replication. In support of the idea that
356 rapid turnover limits PA-X host shutoff activity, the Takimoto group showed that truncation of
357 the pH1N1 PA-X X-ORF to 15 residues in the virus through a premature stop codon increased
358 host shutoff during infection (17). Based on our results, this truncation will also make PA-X
359 more stable. Thus, the link between PA-X stability, host shutoff activity, and virulence should be
360 further studied and rigorously tested during infection.
361
362 Several lines of evidence suggest that PA-X protein turnover is primarily regulated by the X-
363 ORF, including changes in PA-X stability upon X-ORF truncation and aa 220 mutations and
364 destabilization of DsRed by fusion to the X-ORF (Figs 4-5). However, the experiments with
365 chimeric pH1N1 PA-X/PR8 PA-X also suggests a role for the N-terminal RNase domain in
366 regulating PA-X turnover rates (Fig 6). In order to tease apart of the specific contributions of

367 each domain to PA-X turnover rates, a more thorough understanding of the mechanism of PA-X
368 turnover is needed. In a proteomic screen, we identified three components of the proteasome,
369 PSME3, PSMD3, and PSMC5, and the ubiquitin E3 ligase HUWE1 as high-confidence PA-X
370 interacting partners (3). These observations suggest a potential role for proteasomal degradation
371 in PA-X turnover. Determining the mechanism of PA-X turnover in the infected cells and the
372 potential role of the ubiquitin-proteasome system in this process is a current avenue of
373 investigation.
374
375 Since the first 15 amino acids of the X-ORF are sufficient for host shutoff activity (3, 17, 22),
376 why the rest of the X-ORF is retained through evolution has remained unclear. With the
377 exception of a few equine H7N7 and bat influenza strains, all influenza A strains have PA-X
378 with X-ORFs of 41 or 61 amino acids, even though there are earlier positions in the X-ORF
379 where a stop codon could have evolved without changing the PA reading frame (16). Our study
380 suggests that the rest of the X-ORF may be needed to regulate PA-X, and in particular to ensure
381 that PA-X is rapidly turned over. A post-translational mechanism to control PA-X protein levels
382 may be important to limit activity, because in the context of infection PA-X does not cleave its
383 own transcript and thus does not autoregulate its expression (5). This is in contrast to other viral
384 host shutoff RNases like the alphaherpesvirus protein vhs, which is thought to be able to target
385 its own transcript (35). If hyperactive PA-X is detrimental to viral fitness, there may be selective
386 pressure to maintain the instability of PA-X, and thus retain the distal portion of the X-ORF even
387 though it is not required for host shutoff activity.
388
389 It was surprising that the turnover rate of pH1N1 PA-X was dramatically different from that of

390 most other strains (Fig 3). While the biggest difference between pH1N1 and the other tested
391 strains is the absence of the 20 distal amino acids, we find that this truncation is not responsible
392 for the reduced degradation (Fig 4J and 6B-C). PA-X from strains with avian origin PA
393 segments, like that of pH1N1 (36), have been reported to have higher host shutoff activity
394 compared to PA-X from strains with human-adapted PA segments (23). This has raised the
395 possibility that PA-X host shutoff activity is linked to virulence and pathogenicity (37). Given
396 that pH1N1 PA-X accumulates to higher levels in the cell when compared to its counterparts
397 from PR8, Udorn, and HK06 (Fig 1 and 3), which are human-adapted, it is possible that strain-
398 specific differences in PA-X activity may be the result of strain-specific differences in stability.
399 Interestingly, four amino acid changes have arisen in pH1N1 PA-X since after the 2009 pH1N1
400 strain was introduced into humans (24). These changes appear to reduce PA-X host shutoff
401 activity (24). It would be interesting to investigate whether they also affect PA-X stability. In
402 general, it will be important to assess the functional consequences of PA-X stability in terms of
403 PA-X host shutoff activity and viral pathogenesis.
404
405 Collectively our results reveal for the first time that PA-X is markedly unstable. The stability of
406 different PA-X variants may control host shutoff activity, which could have consequences for
407 virulence and pathogenesis. Interestingly, we found that aa 17-41 of the X-ORF contribute to
408 regulation of PA-X stability. Previous sequence analyses have shown that this region is
409 maintained through evolution despite not being required for host shutoff activity. Thus, having
410 an unstable PA-X may be advantageous for the virus and be selected for during evolution.
411 Further elucidation of the mechanism of PA-X turnover in the infected cell and its functional

412 consequences will uncover important aspects of PA-X biology and regulation of host shutoff,

413 allowing us to further link PA-X activity with influenza A virus virulence and pathogenesis.

414 **ACKNOWLEDGEMENTS**

415 We thank Dr. Seema Lakdawala, Dr. Chris Sullivan, Dr. Jesse Bloom and Dr. Richard Webby
416 for constructs, and members of the Moore and Bohm lab and Dr. Malavika Raman for
417 suggestions and feedback. We also thank Dr. Denys Khaperskyy, Dr. Craig McCormick and
418 members of the Gaglia lab for suggestions, feedback, and critical reading of the manuscript. This
419 work was supported by NIH grant R01 AI137358 to M.M.G. R.E.L. was supported by NIH
420 training grant T32 AI007422. S.D.S. is a David J. Cosman, Ph.D. fellow in the Tufts Graduate
421 School of Biomedical Sciences Molecular Microbiology Ph.D. program.

422 **MATERIALS AND METHODS**

423 **Plasmids**

424 pCR3.1-PR8-PA-X-D108A-myc was previously described (5, 38). pCR3.1-PA-X D108A-myc
425 constructs for A/California/7/2009pdm, A/Udorn/307/1972, and A/Hong Kong/218847/2006
426 were generated from the corresponding previously described wild-type plasmids (3, 5) by site-
427 directed mutagenesis. The indicated PA-X coding regions were PCR-amplified using primers in
428 Table 2 and inserted into the SalI and XhoI sites of a pCR3.1-C-terminal-myc backbone.
429 pCR3.1-PA-X-D108A-myc constructs for A/Perth/16/2009 (Perth) was generated by subcloning
430 the PA-X coding region from the plasmid from segment 3 for this strain (a kind gift from Dr.
431 Seema Lakdawala). The Perth PA-X coding region was PCR-amplified using primers in Table 2
432 to delete a base (which mimics the frameshift) and insert the D108A mutation. It was then
433 inserted into the SalI and MluI sites of a pCR3.1-C-terminal-myc backbone. pCR3.1-PR8-PA-
434 X16-D108A-myc and pCR3.1-PR8-PA-X41-D108A-myc were generated by PCR-amplifying
435 the truncated coding region from pCR3.1-PA-X-PR8-D108A-myc using primers in Table 2. The
436 truncated regions were then inserted into the SalI and MluI sites of a pCR3.1-C-terminal-myc
437 backbone. pCR3.1-PR8-PA-X-D108A-R220H-myc and pCR3.1-pH1N1-PA-X-D108A-H220R-
438 myc were generated from the corresponding D108A plasmids by site-directed mutagenesis. The
439 indicated PA-X coding regions were PCR amplified using primers in Table 2 and inserted into
440 the SalI and XhoI sites of pCR3.1-C-terminal-myc backbone. pCR3.1-pH1N1-X61-PA-X-
441 D108A-myc, pCR3.1-pH1N1-PR8-PA-X-D108A-myc, pCR3.1-PR8-pH1N1-PA-X-D108A-myc
442 were generated by amplifying the coding regions from the corresponding D108A plasmids using
443 primers in Table 2 and then inserting the coding sequences into the SalI and XhoI sites of a
444 pCR3.1-C-terminal-myc backbone. pCDNA3.1-dsRed-XORF and pCDNA3.1-dsRed were

445 generated by amplifying the coding regions from the corresponding regions from pCR3.1-PR8-
446 PA-X and pcDNA3.1-dsRed-DR (a kind gift of Chris Sullivan). The regions were then inserted
447 into the AgeI and XhoI site of pCDNA3.1. pTRIPZ-PR8-PA-X-myc-D108A was previously
448 described in (3, 5). Gibson cloning using HiFi assembly mix (New England Biolabs) was used to
449 make all constructs.
450
451 **Cell lines, transfections, and drug treatments**
452 Human embryonic kidney (HEK293T) cells (ATCC) and derivatives, Madin-Darby Canine
453 Kidney (MDCK) cells (ATCC), A549 (ATCC) cells and derivatives were cultured in Dulbecco's
454 modified Eagle's medium (DMEM; Life Technologies) supplemented with 10% fetal bovine
455 serum (Hyclone) and maintained at 37°C in 5% $CO_2$ atmosphere. A549 cell lines expressing PA-
456 X under a doxycycline-inducible promoter (A549-iPA-X_PR8_wt#1 and A549-iPA-
457 X_PR8_D108A#8) were previously described (5). HEK 293T-iPA-X_PR8_D108A were
458 generated by lentiviral transduction using pTRIPZ-PR8-PA-X-myc-D108A. For all half-life
459 experiments, HEK293T cells were plated in 10-cm dishes and transfected with 12 µg total DNA
460 (including 6 µg of PA-X construct) using JetPrime (Polyplus transfection). 6 hours post
461 transfection, cells were transferred to 6-well plates, and one well was set up per indicated time
462 point. For the indicated 2, 4, and 6-hour cycloheximide experiments, HEK293T cells were plated
463 in 2 6-wells for each indicated strain/construct and transfected with 2 µg of DNA (including 1 µg
464 of PA-X/dsRed construct) per well using JetPrime (Polyplus transfection). 6 hours post
465 transfection, the 2 wells for each construct were trypsinized, mixed together, and replated into 2
466 wells. 24 hours post transfection, cells were treated with 200 µg/mL of cycloheximide (Sigma
467 Aldrich) or $dH_2O$ as vehicle control, and collected for RNA and protein isolation at the indicated

468 time points. For experiments using A549 iPA-X cells, cells were treated with 0.5 µg/mL
469 doxycycline (Thermo Fisher) for 14 hours to induce PA-X expression and then 200 µg/mL of
470 cycloheximide (or vehicle control, $dH_2O$) for 2 hours prior to RNA collection. For experiments
471 using HEK293T iPA-X cells, cells were treated with 2.0 µg/mL doxycycline (Thermo Fisher) for
472 6 hours to induce PA-X expression prior to infection and then 200 µg/mL of cycloheximide (or
473 vehicle control, $dH_2O$) for 2 hours prior to protein collection.
474
475 **Viruses and Infections**
476 Wild type influenza A virus A/Puerto Rico/8/1934 H1N1 (PR8) and the mutant PR8 ΔX were
477 generated as previously described in (3) using the 8-plasmid reverse genetic system (39). Viral
478 stocks were produced in MDCK cells and infectious titers were determined by plaque assay in
479 MDCKs using a 1.2% Avicel overlay described in Matrosovich *et al.* (40). Cell monolayers were
480 mock infected or infected with the wild-type or PA-X mutant viruses for 1 hr at 37°C.
481 Monolayers were then washed with PBS, and fresh infection media (0.5% Bovine Serum
482 Albumin (BSA; Sigma Aldrich) in DMEM was added and cells were incubated at 37°C in 5%
483 $CO_2$ atmosphere. For experiments with A549 cells, infection media was supplemented with 0.5
484 µg/mL of L-(tosylamido-2-phenyl) ethyl chloromethyl ketone (TPCK)-treated trypsin) (Sigma
485 Aldrich). For A549 infections, an MOI of 5 was used, and cycloheximide was added to block
486 translation 24 hours after infection. For HEK 293T-iPA-X_PR8_D108A infections, an MOI of 1
487 was used and cycloheximide was added 18 hours after infection.
488
489 **RNA purification, cDNA preparation and RT-qPCR**

490 RNA was extracted from cells and purified using the Quick-RNA Miniprep kit (Zymo Research),
491 following manufacturer's protocol. In all cases, the RNA was treated with Turbo DNase (Life
492 Technologies), then reverse transcribed using iScript supermix (Bio-Rad) per manufacturer's
493 protocol. qPCR was performed using iTaq Universal SYBR Green supermix (Bio-Rad), on the
494 Bio-Rad CFX Connect Real-Time System qPCR and analyzed with Bio-Rad CFX Manager 3.1
495 Program. The primers used are listed in Table 2.
496
497 **Protein extraction, western blotting and antibodies**
498 Total cellular protein was collected in protein lysis buffer (50 mM Tris-HCl pH 7.4, 150 mM
499 NaCl, 2 mM EDTA, 0.5% sodium deoxycholate, 0.5% SDS, 1% NP-40) supplemented with
500 cOmplete EDTA-free protease inhibitor cocktail (Roche) and 1 U/mL benzonase nuclease
501 (Sigma Aldrich). The benzonase is included to degrade DNA and promote release of PA-X from
502 the nucleus. Proteins were separated on 12% SDS-PAGE gels and transferred onto 0.22 μm
503 PVDF membranes (Millipore). Western Blots were performed in PBST with 0.5% milk using
504 antibodies against the Myc tag (1:1000, Cell Signaling Technologies 2276), influenza A virus
505 (1:2000, Abcam ab20841), dsRed (1:200, Santa Cruz Biotechnology sc-101526), human
506 GAPDH (1:1000, Cell Signaling Technologies 5174), and human β-tubulin (1:1000, Cell
507 Signaling Technologies 2128). Secondary antibodies conjugated to HRP were purchased from
508 Southern Biotechnologies (rabbit, OB4030-05; mouse, OB1031-05; goat, OB6106-05) and used
509 at 1:5,000 dilution. Membranes were developed using Pierce ECL Western blotting substrate
510 (Thermo Fisher) and imaged with a Syngene G:Box Chemi XT4 gel doc system. Images were
511 quantified using GeneTools version 4.3.8.0
512

513 **Statistical Analysis**

514 All statistical analysis was performed using GraphPad Prism version 8.0 for Mac OS X,
515 (GraphPad Software, San Diego, CA, USA). For half-life experiments, statistical significance
516 was determined by performing linear regression and comparing slopes and intercepts. For other
517 experiments, statistical significance was determined by Student's *t*-test, or analysis of variance
518 (ANOVA) followed by a *post-hoc* multiple comparisons test (Sidak's or Tukey's) as indicated.
519 All bar graphs are mean +/- standard deviation. A minimum of three biological replicates were
520 conducted for all experiments.

521 **References**


522 1. Jagger BW, Wise HM, Kash JC, Walters K-A, Wills NM, Xiao Y-L, Dunfee RL,
523 Schwartzman LM, Ozinsky A, Bell GL, Dalton RM, Lo A, Efstathiou S, Atkins JF, Firth
524 AE, Taubenberger JK, Digard P. 2012. An Overlapping Protein-Coding Region in
525 Influenza A Virus Segment 3 Modulates the Host Response. Science 337:199–204.

526 2. Levene RE, Gaglia MM. 2018. Host Shutoff in Influenza A Virus: Many Means to an End.
527 Viruses 10:475.

528 3. Gaucherand L, Porter BK, Levene RE, Price EL, Schmaling SK, Rycroft CH, Kevorkian Y,
529 McCormick C, Khaperskyy DA, Gaglia MM. 2019. The Influenza A Virus
530 Endoribonuclease PA-X Usurps Host mRNA Processing Machinery to Limit Host Gene
531 Expression. Cell Reports 27:776-792.e7.

532 4. Chaimayo C, Dunagan M, Hayashi T, Santoso N, Takimoto T. Specificity and functional
533 interplay between influenza virus PA-X and NS1 shutoff activity 26.

534 5. Khaperskyy DA, Schmaling S, Larkins-Ford J, McCormick C, Gaglia MM. 2016. Selective
535 Degradation of Host RNA Polymerase II Transcripts by Influenza A Virus PA-X Host
536 Shutoff Protein. PLOS Pathogens 12:e1005427.

537 6. Gao H, Sun Y, Hu J, Qi L, Wang J, Xiong X, Wang Y, He Q, Lin Y, Kong W, Seng L-G,
538 Sun H, Pu J, Chang K-C, Liu X, Liu J. 2015. The contribution of PA-X to the virulence of
539 pandemic 2009 H1N1 and highly pathogenic H5N1 avian influenza viruses. Scientific
540 Reports 5:8262.

541 7. Gong X-Q, Sun Y-F, Ruan B-Y, Liu X-M, Wang Q, Yang H-M, Wang S-Y, Zhang P,
542 Wang X-H, Shan T-L, Tong W, Zhou Y-J, Li G-X, Zheng H, Tong G-Z, Yu H. 2017. PA-X
543 protein decreases replication and pathogenicity of swine influenza virus in cultured cells
544 and mouse models. Veterinary Microbiology 205:66–70.

545 8. Hayashi T, MacDonald LA, Takimoto T. 2015. Influenza A Virus Protein PA-X
546 Contributes to Viral Growth and Suppression of the Host Antiviral and Immune Responses.
547 Journal of Virology 89:6442–6452.

548 9. Hu J, Mo Y, Wang X, Gu M, Hu Z, Zhong L, Wu Q, Hao X, Hu S, Liu W, Liu H, Liu X,
549 Liu X. 2015. PA-X Decreases the Pathogenicity of Highly Pathogenic H5N1 Influenza A
550 Virus in Avian Species by Inhibiting Virus Replication and Host Response. Journal of
551 Virology 89:4126–4142.

552 10. Xu G, Zhang X, Liu Q, Bing G, Hu Z, Sun H, Xiong X, Jiang M, He Q, Wang Y, Pu J, Guo
553 X, Yang H, Liu J, Sun Y. 2017. PA-X protein contributes to virulence of triple-reassortant
554 H1N2 influenza virus by suppressing early immune responses in swine. Virology 508:45–
555 53.

556 11. Sun Y, Hu Z, Zhang X, Chen M, Wang Z, Xu G, Bi Y, Tong Q, Wang M, Sun H, Pu J,
557 Iqbal M, Liu J. 2020. R195K mutation in the PA-X protein increases the virulence and
558 transmission of influenza A virus in mammalian hosts. J Virol JVI.01817-19,
559 jvi;JVI.01817-19v1.

560 12. Liu L, Song S, Shen Y, Ma C, Wang T, Tong Q, Sun H, Pu J, Iqbal M, Liu J, Sun Y. 2020.
561 Truncation of PA-X Contributes to Virulence and Transmission of H3N8 and H3N2 Canine
562 Influenza Viruses in Dogs. J Virol 94:e00949-20, /jvi/94/15/JVI.00949-20.atom.

563 13. Oishi K, Yamayoshi S, Kozuka-Hata H, Oyama M, Kawaoka Y. 2018. N-Terminal
564 Acetylation by NatB Is Required for the Shutoff Activity of Influenza A Virus PA-X. Cell
565 Reports 24:851–860.

566 14. Oishi K, Yamayoshi S, Kawaoka Y. 2018. Identification of novel amino acid residues of
567 influenza virus PA-X that are important for PA-X shutoff activity by using yeast. Virology
568 516:71–75.

569 15. Firth AE, Jagger BW, Wise HM, Nelson CC, Parsawar K, Wills NM, Napthine S,
570 Taubenberger JK, Digard P, Atkins JF. 2012. Ribosomal frameshifting used in influenza A
571 virus expression occurs within the sequence UCC_UUU_CGU and is in the +1 direction.
572 Open Biology 2:120109.

573 16. Shi M, Jagger BW, Wise HM, Digard P, Holmes EC, Taubenberger JK. 2012. Evolutionary
574 Conservation of the PA-X Open Reading Frame in Segment 3 of Influenza A Virus. Journal
575 of Virology 86:12411–12413.

576 17. Hayashi T, Chaimayo C, McGuinness J, Takimoto T. 2016. Critical Role of the PA-X C-
577 Terminal Domain of Influenza A Virus in Its Subcellular Localization and Shutoff Activity.
578 J Virol 90:7131–7141.

579 18. Košík I, Práznovská M, Košíková M, Bobišová Z, Hollý J, Varečková E, Kostolanský F,
580 Russ G. 2015. The Ubiquitination of the Influenza A Virus PB1-F2 Protein Is Crucial for
581 Its Biological Function. PLoS ONE 10:e0118477.

582 19. Varga ZT, Palese P. 2011. The influenza A virus protein PB1-F2. Virulence 2:542–546.

583 20. Varga ZT, Ramos I, Hai R, Schmolke M, García-Sastre A, Fernandez-Sesma A, Palese P.
584 2011. The Influenza Virus Protein PB1-F2 Inhibits the Induction of Type I Interferon at the
585 Level of the MAVS Adaptor Protein. PLoS Pathog 7:e1002067.

586 21. Varga ZT, Grant A, Manicassamy B, Palese P. 2012. Influenza Virus Protein PB1-F2
587 Inhibits the Induction of Type I Interferon by Binding to MAVS and Decreasing
588 Mitochondrial Membrane Potential. J Virol 86:8359–8366.

589 22. Oishi K, Yamayoshi S, Kawaoka Y. 2015. Mapping of a Region of the PA-X Protein of
590 Influenza A Virus That Is Important for Its Shutoff Activity. Journal of Virology 89:8661–
591 8665.

592 23. Desmet EA, Bussey KA, Stone R, Takimoto T. 2013. Identification of the N-Terminal
593 Domain of the Influenza Virus PA Responsible for the Suppression of Host Protein
594 Synthesis. Journal of Virology 87:3108–3118.

595 24. Nogales A, Martinez-Sobrido L, Chiem K, Topham DJ, DeDiego ML. 2018. Functional
596 Evolution of the 2009 Pandemic H1N1 Influenza Virus NS1 and PA in Humans. Journal of
597 Virology 92:e01206-18.

598 25. Santos A, Pal S, Chacón J, Meraz K, Gonzalez J, Prieto K, Rosas-Acosta G. 2013.
599 SUMOylation Affects the Interferon Blocking Activity of the Influenza A Nonstructural
600 Protein NS1 without Affecting Its Stability or Cellular Localization. Journal of Virology
601 87:5602–5620.

602 26. Cheng Y-Y, Yang S-R, Wang Y-T, Lin Y-H, Chen C-J. 2017. Amino Acid Residues 68–71
603 Contribute to Influenza A Virus PB1-F2 Protein Stability and Functions. Front Microbiol
604 8:692.

605 27. Chen W, M. Smeekens J, Wu R. 2016. Systematic study of the dynamics and half-lives of
606 newly synthesized proteins in human cells. Chemical Science 7:1393–1400.

607 28. Rigby RE, Wise HM, Smith N, Digard P, Rehwinkel J. 2019. PA-X antagonises MAVS-
608 dependent accumulation of early type I interferon messenger RNAs during influenza A
609 virus infection. Sci Rep 9:7216.

610 29. Hara K, Schmidt FI, Crow M, Brownlee GG. 2006. Amino Acid Residues in the N-
611 Terminal Region of the PA Subunit of Influenza A Virus RNA Polymerase Play a Critical
612 Role in Protein Stability, Endonuclease Activity, Cap Binding, and Virion RNA Promoter
613 Binding. Journal of Virology 80:7789–7798.

614 30. Maier HJ, Kashiwagi T, Hara K, Brownlee GG. 2008. Differential role of the influenza A
615 virus polymerase PA subunit for vRNA and cRNA promoter binding. Virology 370:194–
616 204.

617 31. Gao H, Sun H, Hu J, Qi L, Wang J, Xiong X, Wang Y, He Q, Lin Y, Kong W, Seng L-G,
618 Pu J, Chang K-C, Liu X, Liu J, Sun Y. 2015. Twenty amino acids at the C-terminus of PA-

619 X are associated with increased influenza A virus replication and pathogenicity. Journal of
620 General Virology 96:2036–2049.

621 32. Feng KH, Sun M, Iketani S, Holmes EC, Parrish CR. 2016. Comparing the functions of
622 equine and canine influenza H3N8 virus PA-X proteins: Suppression of reporter gene
623 expression and modulation of global host gene expression. Virology 496:138–146.

624 33. Wang X-H. 2020. The role of PA-X C-terminal 20 residues of classical swine influenza
625 virus in its replication and pathogenicity. Veterinary Microbiology 5.

626 34. Adams KW, Cooper GM. 2007. Rapid Turnover of Mcl-1 Couples Translation to Cell
627 Survival and Apoptosis. J Biol Chem 282:6192–6200.

628 35. Elgadi MM, Hayes CE, Smiley JR. 1999. The Herpes Simplex Virus vhs Protein Induces
629 Endoribonucleolytic Cleavage of Target RNAs in Cell Extracts. J Virol 73:7153–7164.

630 36. Garten RJ, Davis CT, Russell CA, Shu B, Lindstrom S, Balish A, Sessions WM, Xu X,
631 Skepner E, Deyde V, Okomo-Adhiambo M, Gubareva L, Barnes J, Smith CB, Emery SL,
632 Hillman MJ, Rivailler P, Smagala J, Graaf M de, Burke DF, Fouchier RAM, Pappas C,
633 Alpuche-Aranda CM, López-Gatell H, Olivera H, López I, Myers CA, Faix D, Blair PJ, Yu
634 C, Keene KM, Dotson PD, Boxrud D, Sambol AR, Abid SH, George KS, Bannerman T,
635 Moore AL, Stringer DJ, Blevins P, Demmler-Harrison GJ, Ginsberg M, Kriner P,
636 Waterman S, Smole S, Guevara HF, Belongia EA, Clark PA, Beatrice ST, Donis R, Katz J,
637 Finelli L, Bridges CB, Shaw M, Jernigan DB, Uyeki TM, Smith DJ, Klimov AI, Cox NJ.
638 2009. Antigenic and Genetic Characteristics of Swine-Origin 2009 A(H1N1) Influenza
639 Viruses Circulating in Humans. Science 325:197–201.

640 37. Lutz MM, Dunagan MM, Kurebayashi Y, Takimoto T. 2020. Key Role of the Influenza A
641 Virus PA Gene Segment in the Emergence of Pandemic Viruses. 4. Viruses 12:365.

642 38. Khaperskyy DA, Emara MM, Johnston BP, Anderson P, Hatchette TF, McCormick C.
643 2014. Influenza A Virus Host Shutoff Disables Antiviral Stress-Induced Translation Arrest.
644 PLOS Pathogens 10:e1004217.

645 39. Hoffmann E, Neumann G, Kawaoka Y, Hobom G, Webster RG. 2000. A DNA transfection
646 system for generation of influenza A virus from eight plasmids. Proceedings of the National
647 Academy of Sciences 97:6108–6113.

648 40. Matrosovich M, Matrosovich T, Garten W, Klenk H-D. 2006. New low-viscosity overlay
649 medium for viral plaque assays. Virol J 3:63.

650

651

652 **FIGURE AND TABLE LEGENDS**

653 **TABLE 1: HALF-LIVES OF PA-X FROM PR8, pH1N1, UDORN, HK06, AND PERTH.** A
654 linear regression was carried out on the quantification plots in Figure 3. The slope of the linear
655 regression line and the calculated half-life are reported. The half-life was calculated as the
656 negative of the inverse of the slope in minutes. The slope and half-life for PR8 PA-X was
657 calculated based on regression analysis from Figure 1B.

658

659 **TABLE 2: PRIMERS USED IN THIS STUDY.** Primers used in this study for RT-qPCR and
660 cloning.

661

662 **FIGURE 1: PA-X is unstable**.
663 (A-C) Protein and RNA samples were collected from HEK293T cells expressing catalytically
664 inactive PR8 PA-X D108A at the indicated time points after treatment with 200 µg/mL of
665 cycloheximide (CHX) to inhibit translation. (-) indicates vehicle-treated cells collected at 120
666 minutes. (A) Representative western blot using anti-myc antibodies to detect myc-tagged PA-X
667 and tubulin as a loading control. (B) Plot of the relative levels of PA-X after cycloheximide
668 treatment. For each replicate, PA-X protein levels were normalized to tubulin protein levels and
669 reported as the $\log_2$ transformed ratio relative to time 0. The line represents the linear regression
670 and the shaded region its 95% confidence interval. n = 7 (C) Levels of PA-X mRNA were
671 measured by RT-qPCR. After normalization to 18S rRNA, levels were plotted as amounts
672 relative to time 0. n = 3.

673

674 **FIGURE 2: PA-X is unstable during infection**

675 (A) Levels of the indicated endogenous RNAs were measured by RT-qPCR in A549 "iPA-X"
676 cells, which express wild-type (wt) PR8 PA-X or a PR8 PA-X catalytic mutant (D108A) under a
677 doxycycline-inducible promoter. RNA samples were collected after 14 hours of PA-X induction
678 with doxycycline followed by a 2-hour treatment with 200 μg/mL of cycloheximide (CHX) or
679 vehicle control. After normalization to 18S rRNA, mRNA levels are plotted relative to
680 uninduced cells for each condition and cell line (G6PD, TAF7) or relative to induced wt iPA-X
681 cells (PA-X). n ≥ 4. (B) Levels of the endogenous human mRNAs (G6PD and TAF7) and viral
682 RNAs (HA) were measured by RT-qPCR in cells infected with wt PR8 or the PA-X-defective
683 PR8 ΔX strain at a MOI of 5 for 24 hours prior to a 2-hour treatment with 200 μg/mL of
684 cycloheximide (CHX) to inhibit translation or a vehicle control. After normalization to 18S
685 rRNA, RNA levels are plotted relative to PR8 ΔX-infected cells for each condition (G6PD,
686 TAF7) or as amounts normalized to cellular 18S rRNA (HA). n = 4. (C-E) Expression of PA-X-
687 myc was induced in HEK293T-iPA-X_PR8_D108A with 2.0 μg/mL doxycycline (dox) for 6
688 hours, followed by either mock or wt PR8 infection at MOI = 1 for 18 hours. Protein samples
689 were collected after a subsequent 2-hour treatment with 200 μg/mL of cycloheximide (CHX) to
690 inhibit translation (+) or with vehicle control (-). (C) Representative western blot using anti-myc
691 antibodies to detect myc-tagged PA-X with tubulin as a loading control and anti-IAV antibodies
692 to detect M1 with GAPDH as a loading control. (D) For each replicate, levels of myc-tagged PA-
693 X were normalized to tubulin protein levels and reported as the amount relative to induced, mock
694 infected, vehicle treated cells. n = 4. (E) For each replicate, levels of M1 were normalized to
695 GAPDH protein levels and reported as the amount relative to wt infected, vehicle treated cells. n
696 = 4. ** = $p < 0.01$, **** = $p < 0.0001$, ns = $p > 0.05$. Significance was calculated using 3-way

697 ANOVA followed by Tukey's multiple comparisons test (A), 2-way ANOVA followed by
698 Sidak's multiple comparisons test (B, D), or Student's t-test (E).
699
700 **FIGURE 3: The half-life of PA-X varies among influenza A virus strains.**
701 Protein and RNA samples were collected from HEK293T cells expressing catalytically inactive
702 (D108A mutant) C-terminally myc tagged PA-X from the indicated strains at the indicated time
703 points after treatment with 200 µg/mL of cycloheximide (CHX) to inhibit translation. (-) denotes
704 vehicle-treated cells collected at 120 minutes (A-F) or 6 hours (G-L). (A, D, G, J) Representative
705 western blots using anti-myc antibodies to detect myc-tagged PA-X and tubulin as a loading
706 control. (B, E, H, K) Plot of the relative levels of PA-X after cycloheximide treatment. For each
707 replicate, PA-X protein levels were normalized to tubulin protein levels and reported as the $\log_2$
708 transformed ratio from time zero. The line represents the linear regression and the shaded region
709 its 95% confidence interval. $n \geq 3$ for each variant. The half-life ($t_{1/2}$) is calculated as the
710 negative inverse of the slope and reported in minutes in the figure and/or in Table 1. For (K), the
711 *p* value is calculated relative to PR8 PA-X (PR8 PA-X: slope = -0.64, confidence interval: -0.75
712 – -0.53; pH1N1 PA-X: slope = -0.29, confidence interval: -0.36 - -0.22). (C, F, I, L) Levels of
713 PA-X mRNA were measured by RT-qPCR. After normalization to 18S rRNA, levels are plotted
714 as amounts relative to time 0. $n \geq 3$.
715
716 **FIGURE 4: Amino acids 17-41 of the X-ORF contribute to regulation of PA-X turnover**
717 (A-C) Protein and RNA samples were collected from HEK293T cells expressing the indicated
718 dsRed variant 6 hours after treatment with 200 µg/mL of cycloheximide (CHX) to inhibit
719 translation (+) or vehicle control (-). (A) Representative western blot using anti-dsRed antibodies

720 to detect dsRed and tubulin as a loading control. (B) For each replicate, dsRed protein levels
721 were normalized to tubulin protein levels and reported as the amount normalized to vehicle
722 control for each dsRed variant. ** = $p < 0.01$, ns = $p > 0.05$, 2-way ANOVA followed by Sidak's
723 multiple comparisons test. n = 3. (C) Levels of dsRed mRNA were measured by RT-qPCR. After
724 normalization to 18S rRNA, levels are plotted as amounts relative to dsRed vehicle control. n =
725 3. (D, H) Schematic diagram of PA-X domains and PR8 PA-X16 (D) or PR8 PA-X41 (H)
726 truncations used. (E-G, I-K) Protein and RNA samples were collected from HEK293T cells
727 expressing the catalytically inactive full-length or the indicated truncated C-terminally myc-
728 tagged PA-X at the indicated time points after treatment with 200 μg/mL of cycloheximide
729 (CHX) to inhibit translation. (-) indicates vehicle-treated cells collected at 120 minutes. (E, I)
730 Representative western blot using anti-myc antibodies to detect myc-tagged PA-X and tubulin as
731 a loading control. (F, J) Plot of the relative levels of PA-X after cycloheximide treatment. For
732 each replicate, PA-X protein levels were normalized to tubulin protein levels and reported as the
733 $\log_2$ transformed ratio from time 0. A linear regression was performed for each dataset and the *p*
734 value calculated relative to PR8 PA-X61 (full length PA-X). The lines represent the linear
735 regression and the shaded regions indicate the 95% confidence interval (F: PA-X61: slope = -
736 0.72, confidence interval = -1.05 – -0.39; PA-X16: slope = 0.33, confidence interval = 0.03 –
737 0.63; J: PA-X61: slope = -0.58; confidence interval: -0.87 – -0.28; PA-X41: slope = -0.61,
738 confidence interval = -0.84 – -0.38). The half-lives ($t_{1/2}$) were calculated as the negative inverse
739 of the slope and are reported in minutes. As the slope for PA-X16 is positive, the half-life of this
740 protein cannot be calculated and is therefore reported as longer than the time course of the
741 experiment. n ≥ 3 (G, K) Levels of the mRNAs for the indicated truncated PA-X were measured

742 by RT-qPCR. After normalization to 18S rRNA, levels are plotted as amounts relative to time 0.
743 n > 3.
744
745 **Figure 5: PA-X aa 220 plays a role in protein turnover**
746 (A) Alignment of the X-ORF of PA-X from PR8, Udorn, HK06, Perth, and pH1N1. The zoomed
747 in region shows aa 17-41 of the X-ORF (PA-X aa 208-232). Residue 220 is boxed. * = same
748 residue, : = strong similarity, . = weak similarity. (B-G) Protein and RNA samples were collected
749 from HEK293T cells expressing the indicated catalytically inactive C-terminally myc-tagged
750 PA-X variant 2 hours after treatment with 200 µg/mL of cycloheximide (CHX) to inhibit
751 translation (+) or vehicle control (-). (B, E) Representative western blot using anti-myc
752 antibodies to detect myc-tagged PA-X with tubulin as a loading control. (C, F) For each
753 replicate, PA-X protein levels were normalized to tubulin protein levels and reported as the
754 amount normalized to vehicle control for each variant. *** = $p < 0.001$, ns = $p > 0.05$, 2-way
755 ANOVA followed by Sidak's multiple comparisons test. n ≥ 3. (D, G) Levels of PA-X mRNA
756 were measured by RT-qPCR. After normalization to 18S rRNA, levels are plotted as amounts
757 normalized to vehicle control treated cells expressing the wt variant. n ≥ 3.
758
759 **Figure 6: The N-terminal domain of PA-X also has a role in PA-X stability**
760 (A) Schematic diagram of the PR8/pH1N1 PA-X chimeras used. (B-G) Protein and RNA
761 samples were collected from HEK293T cells expressing the indicated catalytically inactive C-
762 terminally myc-tagged PA-X variant 2 hours after treatment with 200 µg/mL of cycloheximide
763 (CHX) to inhibit translation (+) or vehicle control (-). (B, E) Representative western blot using
764 anti-myc antibodies to detect myc-tagged PA-X and tubulin as a loading control. (C, F) For each

765 replicate, PA-X protein levels were normalized to tubulin protein levels and reported as the
766 amount normalized to vehicle control for each variant. n = 4 (D, G) Levels of PA-X mRNA were
767 measured by RT-qPCR. After normalization to 18S rRNA, levels are plotted as amounts relative
768 to vehicle-treated cells for each variant. n = 3. **** = $p < 0.0001$, ns = $p > 0.05$, 2-way ANOVA
769 followed by Sidak's multiple comparisons test.

770 **Table 1: Half-lives of PA-X from PR8, pH1N1, Udorn, HK06, and Perth**

| PA-X | Slope of linear regression | Half-Life in Minutes | 95% confidence interval on slope |
|---|---|---|---|
| A/Puerto Rico/8/1934 | -0.70 | 86 | -0.90 to -0.50 |
| A/California/7/2009pdm pH1N1 | -0.29 | 207 | -0.36 to -0.22 |
| A/Udorn/307/1973 H3N2 | -1.77 | 34 | -2.41 to -1.14 |
| A/Perth/16/2009 H3N2 | -0.39 | 156 | -0.48 to -0.29 |
| A/Hong Kong/218847/2006 H1N1 | -0.73 | 83 | -1.07 to -0.38 |

771

772 **Table 2: Primers used in this study**

| Purpose | Sequence (5’ - 3’) |
|---|---|
| 18S qPCR Forward | GTAACCCGTTGAACCCCATT |
| 18S qPCR Reverse | CCATCCAATCGGTAGTAGCG |
| PA-X qPCR Forward- amplifies BGH 3’ UTR region on the vector (Fig 1, 3, 4) | GAGTCTAGAGGGCCCGTTTA |
| PA-X qPCR Reverse- amplifies BGH 3’ UTR region on the vector (Fig 1, 3, 4) | GAGGGGCAAACAACAGATGG |
| PR8 PA-X qPCR Forward - Fig 2, 5, 6-PR8, PR8-pH1N1 | GCGACAATGCTTCAATCCGA |
| PR8 PA-X qPCR Reverse - Fig 2, 5, 6-PR8, PR8-pH1N1 | TTGACTCGCCTTGCTCATTG |
| pH1N1 PA-X qPCR Forward – Fig 5, 6-pH1N1, pH1N1-X61, pH1N1-PR8 | GTCAGTCCGAAAGAGGCGAA |
| pH1N1 PA-X qPCR Reverse – Fig 5, 6-pH1N1, pH1N1-X61, pH1N1-PR8 | AAGGCTGGAGAAGTTCGGTG |
| HA qPCR Forward | CTGGACCTTGCTAAAACCCG |
| HA qPCR Reverse | TCTGGAAAGGGAGACTGCTG |
| G6PD qPCR Forward | TGAGCCAGATAGGCTGGAA |

| | |
|---|---|
| G6PD qPCR Reverse | TAACGCAGGCGATGTTGTC |
| TAF7 qPCR Forward | TAGCACTGATCCTAAAGCAAGC |
| TAF7 qPCR Reverse | GGCAGAGTAATTCCGTGGTTC |
| dsRed qPCR Forward | GATCCACAAGGCCCTGAAGC |
| dsRed qPCR Reverse | GCTCCACGATGGTGTAGTCC |
| Clone PA-X Variants -amplifies CDS starting from 5' end vector sequences to clone into pCR3.1 SalI site | CTTAAGCTTGGTACCGGAGTACTGG |
| Clone PA-X Variants -amplifies CDS at BGH 3' UTR to clone into pCR3.1 XhoI site | GTTTAAACGGGCCCTCTAGACTCGA |
| Make D108A A/HongKong/218847/2006 - mutates active site (Fwd) | CAGAGCTGGCAGAAACTTTGGTTTCTC AGCT |
| Make D108A A/HongKong/218847/2006 - mutates active site (Rev) | GCCAGCTCTGTATGATTACAAAGAGAA TAGA |
| Make D108A A/California/7/2009pdm- mutates active site (Fwd) | GTCATACAAAGCAGGAAGAAATTTAG GCTTC |
| Make D108A A/California/7/2009pdm- mutates active site (Rev) | TTTCTTCCTGCTTTGTATGACTACAAAG AG |
| Make D108A A/Udorn/307/1972-mutates active site (Fwd) | ATCATACAAAGCTGGCAGAAACTTCGG |
| Make D108A A/Udorn/307/1972-mutates active site (Rev) | GTTTCTGCCAGCTTTGTATGATTACAA GG |
| Clone A/Perth/16/2009 PA-X (wt and D108A) - amplifies from 5' UTR to clone into pCR3.1 SalI site | TAAACTTAAGCTTGGTACCGGAGTACT GGTCGACCCTCCG |
| Make D108A A/Perth/16/2009 - mutates active site (Rev) | AATCATACAAAGCTGGTAGAAACTTCG G |
| Make D108A A/Perth/16/2009 - mutates active site (Fwd) | TTTCTACCAGCTTTGTATGATTACAAGG AG |
| Clone A/Perth/16/2009 PA-X (wt and D108A) - inserts deletion for frameshifting (Rev) | GGACTGACGAAGGAATCCCATAGG |
| Clone A/Perth/16/2009 PA-X (wt and D108A) - inserts deletion for frameshifting (Fwd) | CCTATGGGATTCCTTCGTCAGTCC |

| | |
|---|---|
| Clone Make D108A A/Perth/16/2009 PA-X (wt and D108A) - amplifies at end of CDS to clone into pCR3.1 MluI site | CTGAGATCAGCTTCTGCTCCACGCGTGACTTCTTTGGACATTTGAGAAAGCTTGC |
| Make PR8 PA-X15 - amplifies at 3' end of truncated CDS to clone into pCR3.1 MluI site | ATCAGCTTCTGCTCCACGCGTGATTTCAAACCTTTCTTCAATTG |
| Make PR8 PA-X41 - amplifies at 3' end of truncated CDS to clone into pCR3.1 MluI site | ATCAGCTTCTGCTCCACGCGTGACATAGGCTCTAAAATTTTCAA |
| Make pcDNA3.1-dsRed and pcDNA3.1-dsRed-XORF – amplifies 5' of dsRed to clone into pcDNA3.1 AgeI site | AGCTCGGATCCACCGGTCGCCACCATGGCCTCCTCCGAGGACGTCA |
| Make pcDNA3.1-dsRed – amplifies 3' of dsRed to clone into pcDNA3.1 XhoI site | AACGGGCCCTCTAGACTCGAGTCACAGGAACAGGTGGTGGCGGCC |
| Make pcDNA3.1-dsRed-XORF – amplifies 3' of dsRed | CTCGGACTGACGCCTCCACCCAGGAACAGGT |
| Make pcDNA3.1-dsRed-XORF- amplifies 5' of PR8 X-ORF | GGTGGAGGCGTCAGTCCGAGAGAGGAGAAGAGA |
| Make pcDNA3.1-dsRed-XORF- amplifies 3' of PR8 X-ORF to clone into pcDNA3.1 XhoI site | GGCCCTCTAGACTCGAGTCACTTCTTTGGACATTTGAGACA |
| Make pCR3.1-pH1N1-PA-X-D108A-H220R – mutates 220$^{th}$ residue | TCGGCGGGAGACTTTGGTCGGCAAGCTTGCG |
| Make pCR3.1-pH1N1-PA-X-D108A-H220R – mutates 220$^{th}$ residue | TCTCCCGCCGAACTTCTCCAGCCTTGAAAAC |
| Make pCR3.1-PR8-PA-X-D108A-R220H – mutates 220$^{th}$ residue | CGGTGGGAGACTTTGGTCGGCAAGCTTACGC |
| Make pCR3.1-PR8-PA-X-D108A-R220H – mutates 220$^{th}$ residue | TCTCCCACCGAACTTCTCCAGCCTTGAAAAT |
| Make pCR3.1-pH1N1-X61-PA-X-D108A – amplifies 3' of pH1N1 PA-X | AATCCATCCACATAGGCTCTAAAGTTTTCAA |
| Make pCR3.1-pH1N1-X61-PA-X-D108A – amplifies 5' of PR8 20 C terminal residues | AGAGCCTATGTGGATGGATTCGAACCGAACGG |
| Make pCR3.1-pH1N1-PR8-PA-X-D108A – amplifies 3' of pH1N1 PA-X N terminus | TCGGACTGACGAAGGAATCCCATAGACTCCT |

| | |
|---|---|
| Make pCR3.1-pH1N1-PR8-PA-X-D108A – amplifies 5’ of PR8 PA-X X-ORF | GGATTCCTTCGTCAGTCCGAGAGAGGA GAAGAGAC |
| Make pCR3.1-PR8-pH1N1-PA-X-D108A – amplifies 3’ of PR8 PA-X N terminus | TCGGACTGACGAAGGAATCCCAGAGG CCTCT |
| Make pCR3.1-PR8-pH1N1-PA-X-D108A – amplifies 5’ of pH1N1 PA-X X-ORF | GGATTCCTTCGTCAGTCCGAAAGAGGC GAAGAG |

773

**Figure 1**

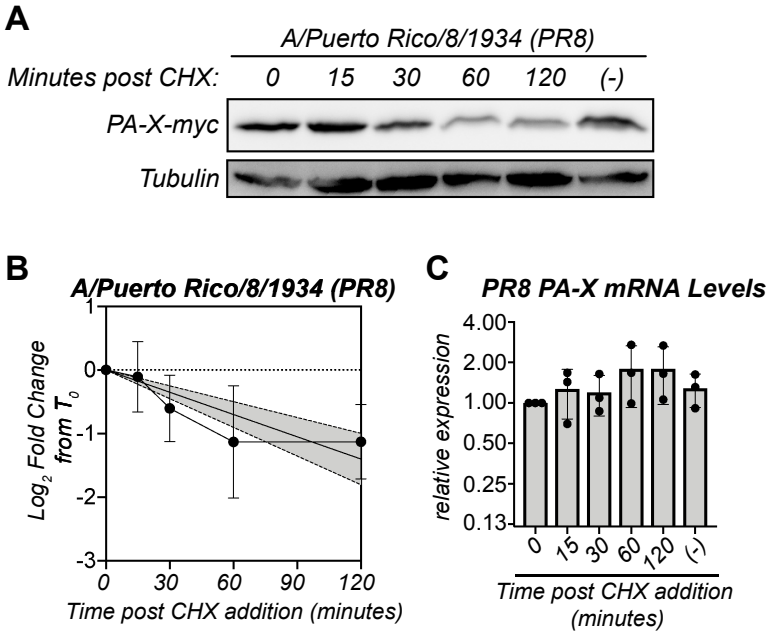


**FIGURE 1: PA-X is unstable.** (A-C) Protein and RNA samples were collected from HEK293T cells expressing catalytically inactive PR8 PA-X D108A at the indicated time points after treatment with 200 µg/mL of cycloheximide (CHX) to inhibit translation. (-) indicates vehicle-treated cells collected at 120 minutes. (A) Representative western blot using anti-myc antibodies to detect myc-tagged PA-X and tubulin as a loading control. (B) Plot of the relative levels of PA-X after cycloheximide treatment. For each replicate, PA-X protein levels were normalized to tubulin protein levels and reported as the log2 transformed ratio relative to time 0. The line represents the linear regression and the shaded region its 95% confidence interval. n = 7 (C) Levels of PA-X mRNA were measured by RT-qPCR. After normalization to 18S rRNA, levels were plotted as amounts relative to time 0. n = 3.

# Figure 2

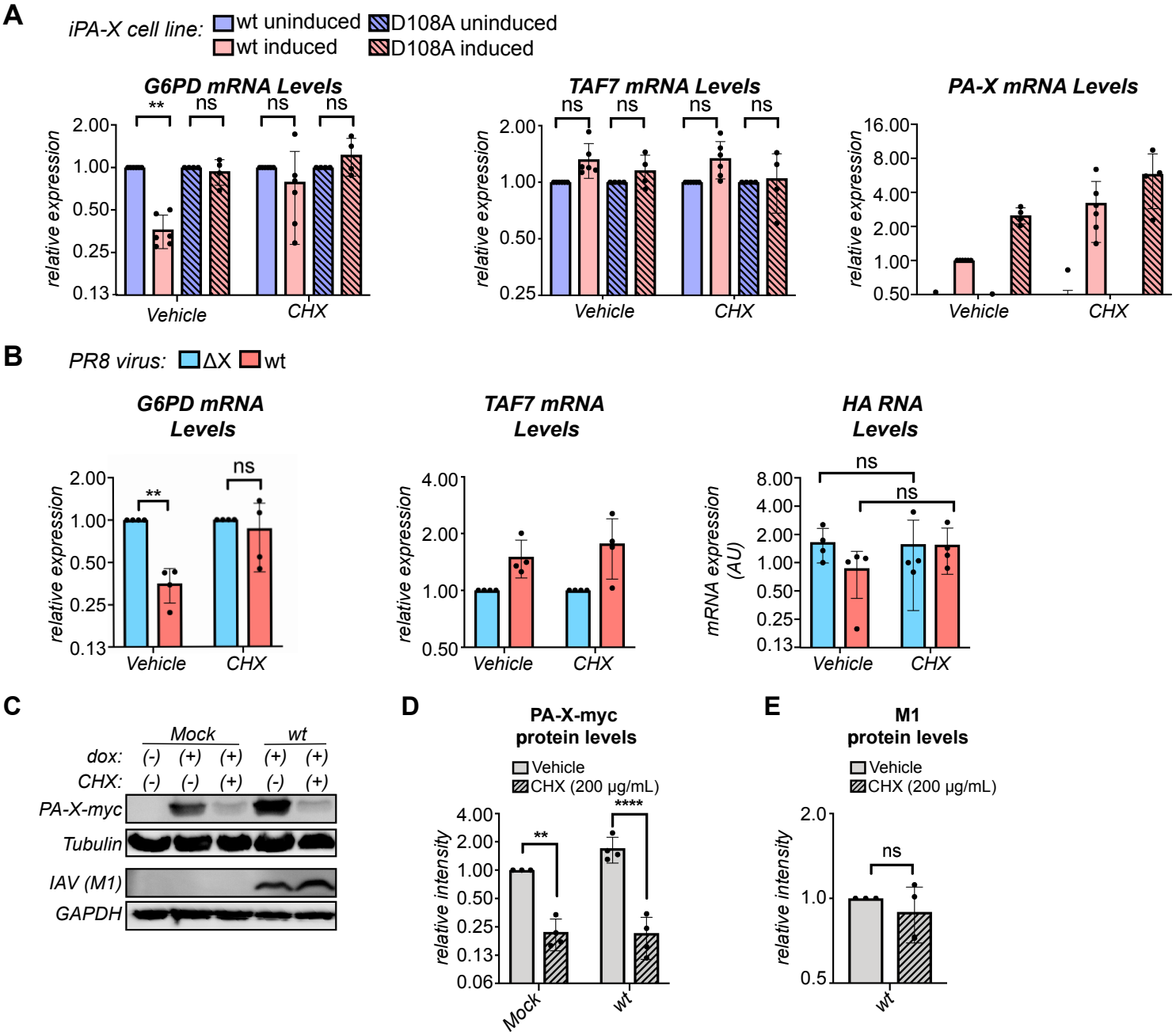


**FIGURE 2: PA-X is unstable during infection.** (A) Levels of the indicated endogenous RNAs were measured by RT-qPCR in A549 "iPA-X" cells, which express wild-type (wt) PR8 PA-X or a PR8 PA-X catalytic mutant (D108A) under a doxycycline-inducible promoter. RNA samples were collected after 14 hours of PA-X induction with doxycycline followed by a 2-hour treatment with 200 μg/mL of cycloheximide (CHX) or vehicle control. After normalization to 18S rRNA, mRNA levels are plotted relative to uninduced cells for each condition and cell line (G6PD, TAF7) or relative to induced wt iPA-X cells (PA-X). n > 3. (B) Levels of the indicated endogenous human mRNAs (G6PD and TAF7) and viral RNAs (HA) were measured by RT-qPCR in cells infected with wt PR8 or the PA-X-defective PR8 ΔX strain at a MOI of 5 for 24 hours prior to a 2-hour treatment with 200 μg/mL of cycloheximide (CHX) to inhibit translation or a vehicle control. After normalization to 18S rRNA, RNA levels are plotted relative to PR8 ΔX-infected cells for each condition (G6PD, TAF7) or as amounts normalized to cellular 18S rRNA (HA). n = 4. (C-E) Expression of PA-X-myc was induced in HEK293T-iPA-X_PR8_D108A with 2.0 μg/mL doxycycline (dox) for 6 hours, followed by either mock or wt PR8 infection at MOI = 1 for 18 hours. Protein samples were collected after a subsequent 2-hour treatment with 200 μg/mL of cycloheximide (CHX) to inhibit translation (+) or with vehicle control (-). (C) Representative western blot using anti-myc antibodies to detect myc-tagged PA-X with tubulin as a loading control and anti-IAV antibodies to detect M1 with GAPDH as a loading control. (D) For each replicate, levels of myc-tagged PA-X were normalized to tubulin protein levels and reported as the amount relative to induced, mock infected, vehicle treated cells. n =4. (E) For each replicate, levels of M1 were normalized to GAPDH protein levels and reported as the amount relative to wt infected, vehicle treated cells. n = 4. ** = $p < 0.01$, **** = $p < 0.0001$, ns = $p > 0.05$. Significance was calculated using 3-way ANOVA followed by Tukey's multiple comparisons test (A), 2-way ANOVA followed by Sidak's multiple comparisons test (B, D), or Student's t-test (E).

## Figure 3

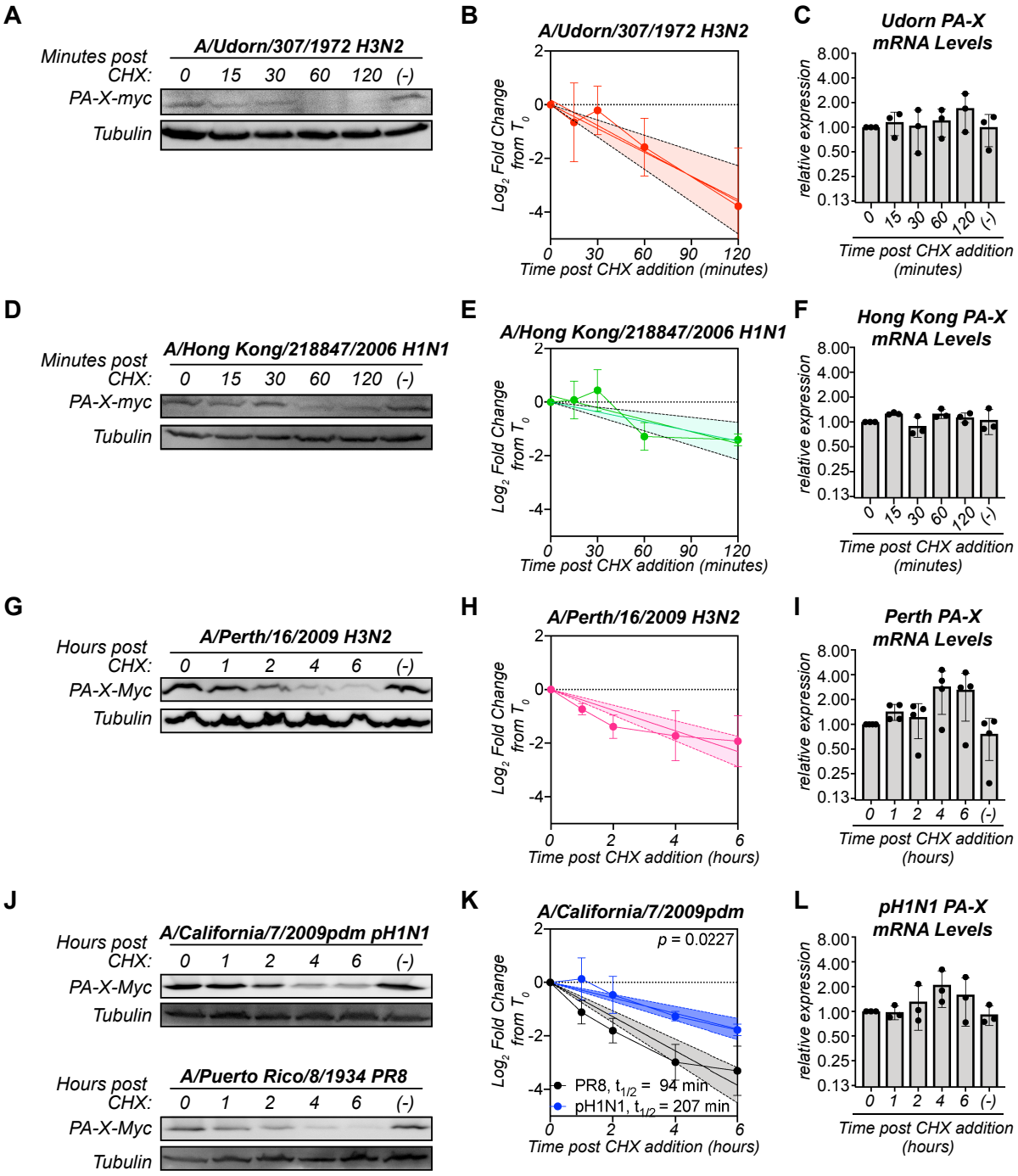


**FIGURE 3: The half-life of PA-X varies among influenza A virus strains.** Protein and RNA samples were collected from HEK293T cells expressing catalytically inactive (D108A mutant) C-terminally myc tagged PA-X from the indicated strains at the indicated time points after treatment with 200 µg/mL of cycloheximide (CHX) to inhibit translation. (-) denotes vehicle-treated cells collected at 120 minutes (A-F) or 6 hours (G-L). (A, D, G, J) Representative western blots using anti-myc antibodies to detect myc-tagged PA-X and tubulin as a loading control. (B, E, H, K) Plot of the relative levels of PA-X after cycloheximide treatment. For each replicate, PA-X protein levels were normalized to tubulin protein levels and reported as the log2 transformed ratio from time zero. The line represents the linear regression and the shaded region its 95% confidence interval. n  3 for each variant. The half-life (t1/2) is calculated as the negative inverse of the slope and reported in minutes in the figure and/or in Table 1. For (K), the p value is calculated relative to PR8 PA-X (PR8 PA-X: slope = -0.64, confidence interval: -0.75 – -0.53; pH1N1 PA-X: slope = -0.29, confidence interval: -0.36 - -0.22). (C, F, I, L) Levels of PA-X mRNA were measured by RT-qPCR. After normalization to 18S rRNA, levels are plotted as amounts relative to time 0. n ≥ 3.

# Figure 4

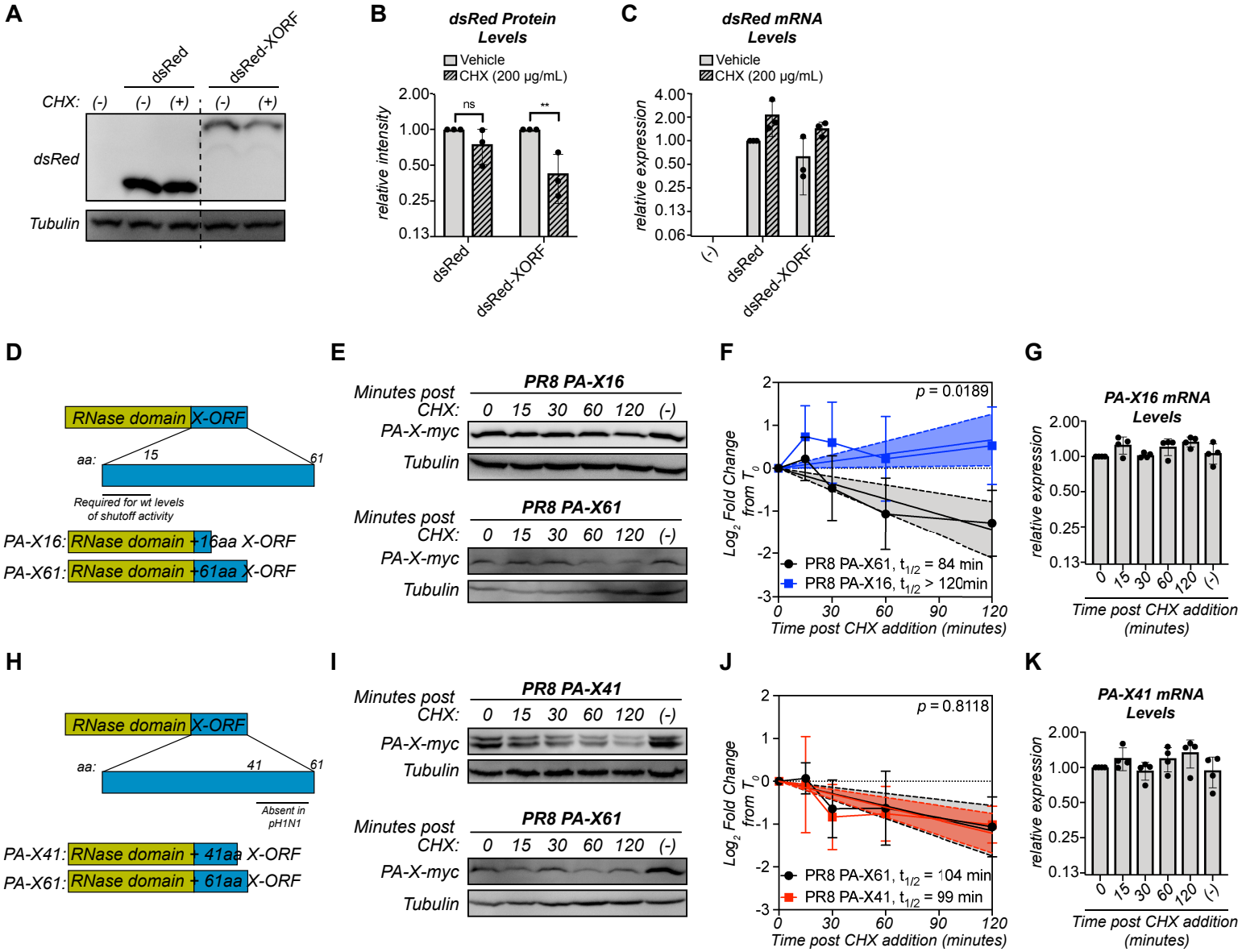


**FIGURE 4: Amino acids 17-41 of the X-ORF contribute to regulation of PA-X turnover.** (A-C) Protein and RNA samples were collected from HEK293T cells expressing the indicated dsRed variant 6 hours after treatment with 200 µg/mL of cycloheximide (CHX) to inhibit translation (+) or vehicle control (-). (A) Representative western blot using anti-dsRed antibodies to detect dsRed and tubulin as a loading control. (B) For each replicate, dsRed protein levels were normalized to tubulin protein levels and reported as the amount normalized to vehicle control for each dsRed variant. ** = $p < 0.01$, ns = $p > 0.05$, 2-way ANOVA followed by Sidak's multiple comparisons test. n = 3. (C) Levels of dsRed mRNA were measured by RT-qPCR. After normalization to 18S rRNA, levels are plotted as amounts relative to dsRed vehicle control. n = 3. (D, H) Schematic diagram of PA-X domains and PR8 PA-X16 (D) or PR8 PA-X41 (H) truncations used. (E-G, I-K) Protein and RNA samples were collected from HEK293T cells expressing the catalytically inactive full-length or the indicated truncated C-terminally myc-tagged PA-X at the indicated time points after treatment with 200 µg/mL of cycloheximide (CHX) to inhibit translation. (-) indicates vehicle-treated cells collected at 120 minutes. (E, I) Representative western blot using anti-myc antibodies to detect myc-tagged PA-X and tubulin as a loading control. (F, J) Plot of the relative levels of PA-X after cycloheximide treatment. For each replicate, PA-X protein levels were normalized to tubulin protein levels and reported as the log2 transformed ratio from time 0. A linear regression was performed for each dataset and the p value calculated relative to PR8 PA-X61 (full length PA-X). The lines represent the linear regression and the shaded regions indicate the 95% confidence interval (F: PA-X61: slope = -0.72, confidence interval = -1.05 – -0.39; PA-X16: slope = 0.33, confidence interval = 0.03 – 0.63; J: PA-X61: slope = -0.58; confidence interval: -0.87 – -0.28; PA-X41: slope = -0.61, confidence interval = -0.84 – -0.38). The half-lives (t1/2) were calculated as the negative inverse of the slope and are reported in minutes. As the slope for PA-X16 is positive, the half-life of this protein cannot be calculated and is therefore reported as longer than the time course of the experiment. n ≥ 3 (G, K) Levels of the mRNAs for the indicated truncated PA-X were measured by RT-qPCR. After normalization to 18S rRNA, levels are plotted as amounts relative to time 0. n > 3.

# Figure 5

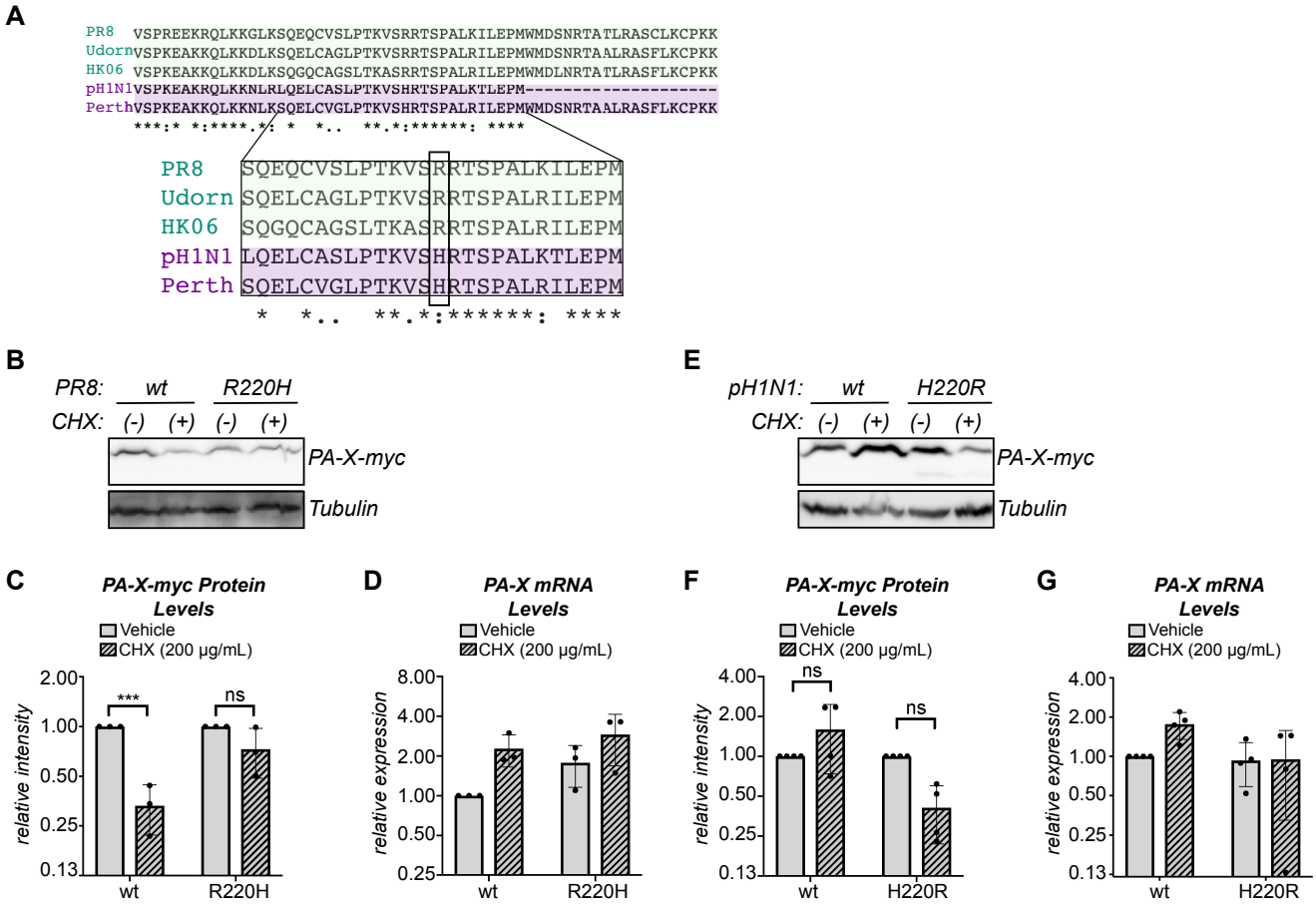


**Figure 5: PA-X aa 220 plays a role in protein turnover.** (A) Alignment of the X-ORF of PA-X from PR8, Udorn, HK06, Perth, and pH1N1. The zoomed in region shows aa 17-41 of the X-ORF (PA-X aa 208-232). Residue 220 is boxed. * = same residue, : = strong similarity, . = weak similarity. (B-G) Protein and RNA samples were collected from HEK293T cells expressing the indicated catalytically inactive C-terminally myc-tagged PA-X variant 2 hours after treatment with 200 µg/mL of cycloheximide (CHX) to inhibit translation (+) or vehicle control (-). (B, E) Representative western blot using anti-myc antibodies to detect myc-tagged PA-X with tubulin as a loading control. (C, F) For each replicate, PA-X protein levels were normalized to tubulin protein levels and reported as the amount normalized to vehicle control for each variant. *** = $p < 0.001$, ns = $p > 0.05$, 2-way ANOVA followed by Sidak's multiple comparisons test. $n \geq 3$. (D, G) Levels of PA-X mRNA were measured by RT-qPCR. After normalization to 18S rRNA, levels are plotted as amounts normalized to vehicle control treated cells expressing the wt variant. $n \geq 3$.

# Figure 6

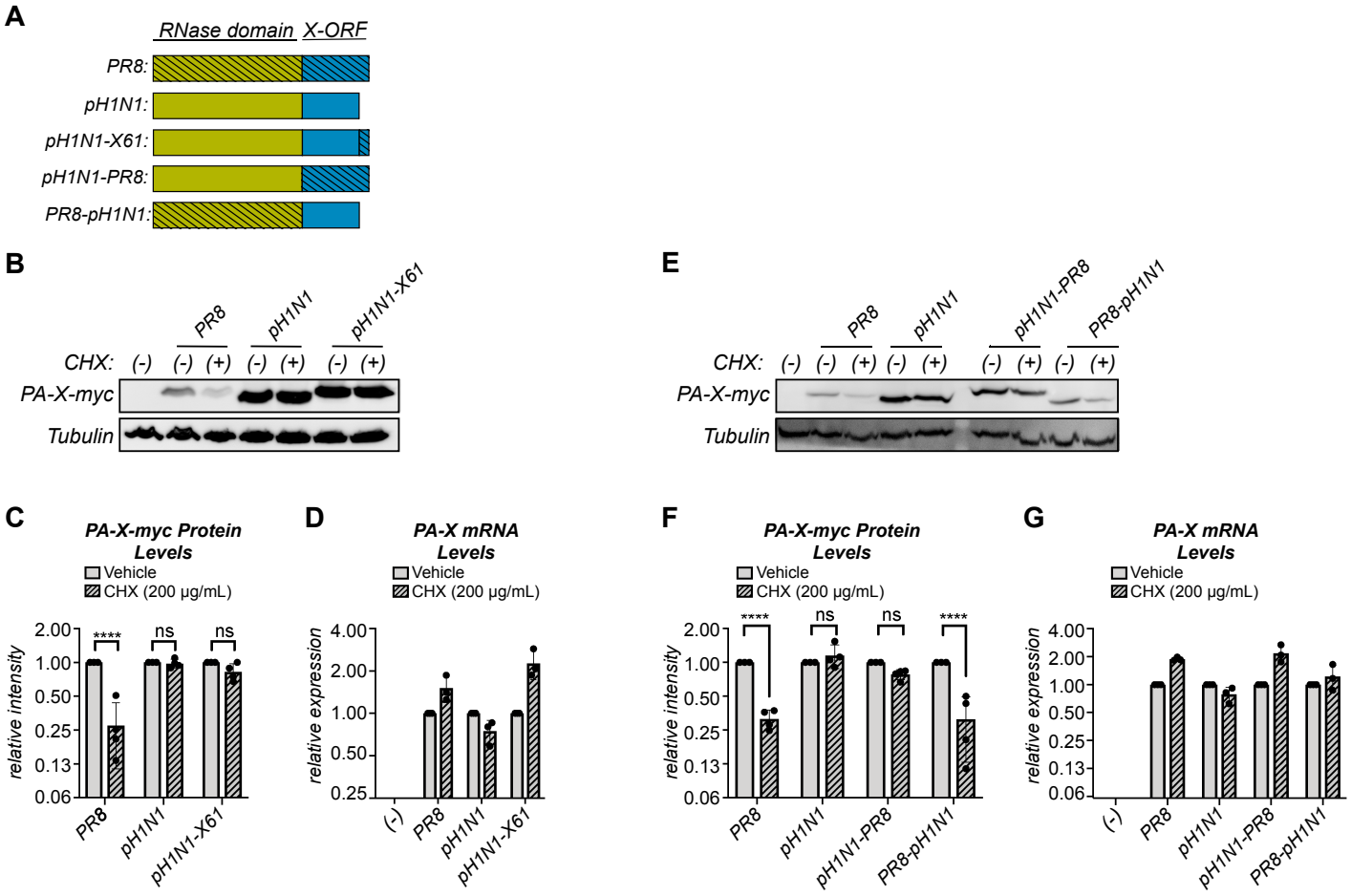


**Figure 6: The N-terminal domain of PA-X also has a role in PA-X stability.** (A) Schematic diagram of the PR8/pH1N1 chimeras used. (B-G) Protein and RNA samples were collected from HEK293T cells expressing the indicated catalytically inactive C-terminally myc-tagged PA-X variant 2 hours after treatment with 200 µg/mL of cycloheximide (CHX) to inhibit translation (+) or vehicle control (-). (B, E) Representative western blot using anti-myc antibodies to detect myc-tagged PA-X and tubulin as a loading control. (C, F) For each replicate, PA-X protein levels were normalized to tubulin protein levels and reported as the amount normalized to vehicle control for each variant. n = 4 (D, G) Levels of PA-X mRNA were measured by RT-qPCR. After normalization to 18S rRNA, levels are plotted as amounts relative to vehicle-treated cells for each variant. n = 3. **** = $p < 0.0001$, ns = $p > 0.05$, 2-way ANOVA followed by Sidak's multiple comparisons test.